

Cracks length OF AA7075 measurement under electrical potential drop technique

Marwa S. Mahammed*, Saad T. Faris

Department of Mechanical Engineering, College of Engineering, University of Diyala, 32001 Diyala, Iraq

*Corresponding author E-mail: eng_grand-mech022@gmail.com

ABSTRACT

In the application of linear elastic fracture mechanics (LEFM) theory to practice, the stress intensity factor (SIF) is the most important element. It's useful for determining if a machine or structural component with a fracture is safe or reliable. It allows you to calculate the crack development rate of a component under fatigue loading, stress corrosion, and other conditions. The primary experimental results for fatigue fracture identification utilizing the Electrical Potential Drop methodology (EPD) under constant load amplitude are presented in this work. Using flat fatigue specimens made of aluminum alloy 7075-T6, the potential drop electrical circuit was conceived, produced, and tested. The experimental findings revealed that the electrical potential drop circuit was capable of detecting the fatigue crack during the test and that the crack length findings were good when compared to the real lengths for fatigue long cracks. The majority of cracks were found in an experiment by measuring crack length after 20% of total fatigue life, so that the remaining fatigue life was > 70% Long cracks or fracture propagation are the most common types of cracks. The goal of this study is to apply the EPD technique to analyze cracks, then extract the S-N curve and compare it to the fatigue test device's results.

KEYWORDS

AA7075 –T6; EPD; Crack length

INTRODUCTION

The rising necessity for the analysis of fatigue damage initiation and propagation under realistic multiaxial fatigue loading scenarios has resulted from the adoption of damage tolerance design principles and increased need for accurate residual fatigue life estimates of aircraft structures. Multiple reasons can cause multiaxiality, including multiaxial external loads, complicated geometry, residual stresses, fracture orientation, and so on. Crack development under pure mode I and/or mode II stress circumstances is the topic of several research papers in the literature [1-4]. In order to characterize material behavior and determine the residual existence of structural materials, accurate laboratory measurements of crack initiation and development are critical. One of the most common techniques for conducting these calculations in metals is the Potential Drop (PD) technique. It is based on the idea that a constant current flowing through a specimen with a crack produces an electrical field that is responsive to changes in the specimen's geometry, especially crack extension.

The PD, which is weighed by two probes on each side of the crack, will rise as the crack expands. This rise in PD can be linked to crack extension with the help of a suitable calibration function. Strain will cause errors in PD measurements as a result of a combination of local crack tip blunting and global specimen deformation [5-7]. It is important to discern the difference in PD caused by crack growth in order to reliably calculate crack initiation and growth in the laboratory. This necessitates an understanding of how other variables, such as strain and crack morphology, affect PD over the course of a test. To observe and quantify fatigue fractures, a variety of techniques may be used. The optical microscope [8] for direct observation, the ultrasonic technique [9], the duplication technique [10], and the Electrical Potential Drop calculation both use high frequency waves sent from a transducer onto a research specimen (EPD). The possible drop (EPD) and Johnson with the experimental

were used to monitor the center-cracked plate, and it was concluded that the EPD measurements of cracks are well agreed with the experimental and Johnson system data [11].

Elhoucine Madhi discovered that the directional (EPD) system has a high sensitivity and can detect elastic and plastic strains as low as 0.05 percent [12]. Matthias Verstraete used 3D elastic-plastic finite element simulations to compare unloading conformity and direct current potential decline (DCPD). The DCPD was discovered to be an effective tool for detecting and calculating crack time [13]. The direct current potential drop (DCPD) sensor was used to measure the duration and depth of very small surface cracks. Masumi S. found that the possible drop imaging technique has a strong capacity for evaluating the fatigue fracture [14]. Potential drop (PD) measuring technology has been further improved to measure thousands of times through each load cycle with high precision to enhance resolution of in-situ assessment of fracture closure and opening in fatigue. The method was used to fatigue crack growth experiments on aluminum 2024-T3 CCT specimens at various maximum stresses and stress ratios, demonstrating that PD may be linked to the development of plasticity and fracture opening and closure. As a result, the approach enables for in-situ measurement of fracture opening and closure stresses in fatigue crack development experiments [15]. The goal is to measure the cracks using the EPD method, extract the S-N curve, and compare it to the fatigue tester results.

THE ELECTRICAL POTENTIAL DROP TECHNIQUE

Direct Current Potential Drop (DCPD) and Alternating Current Potential Drop (ACPD) are the two major variations of the PD strategy (ACPD). Low frequency and high frequency ACPD are two different types of ACPD. The current density decreases exponentially with distance from the surface when an Alternating Current (AC) with a sufficiently high frequency passes through a conductor [16]. The most widely used technique for determining crack length in laboratory specimens made of electrically conductive materials such as aluminum alloys is the electrical Potential Drop (EPD) process. The Direct Current Potential Drop (DCPD) is the most common type of this technique because of its simplicity; however, it requires a lot of current and is subject to a lot of noise. Two injection probes add a steady current to the specimen, while two independent sensing probes calculate the potential decrease around the crack, and a calibration curve is used to infer the crack duration from the EPD figure (1). Analytical, computational, and mathematical approaches can both be used to construct the calibration curve. This approach is based on the fact that any cut in the current carrying body would cause disruptions in the electric potential field. The scale and shape of the discontinuity have a strong impact on the frequency of the disruption. A constant current (maintained constant externally, in this case by constant current supply) is passed through a test specimen for the purpose of crack length tracking. The uncracked cross sectional area of the specimen reduces as the crack duration increases, resulting in an increase in electrical resistance [17]. The EPD performance readings are influenced by the thickness of the specimen. The crack was oriented in the same direction as the current flowing through the specimen being examined.

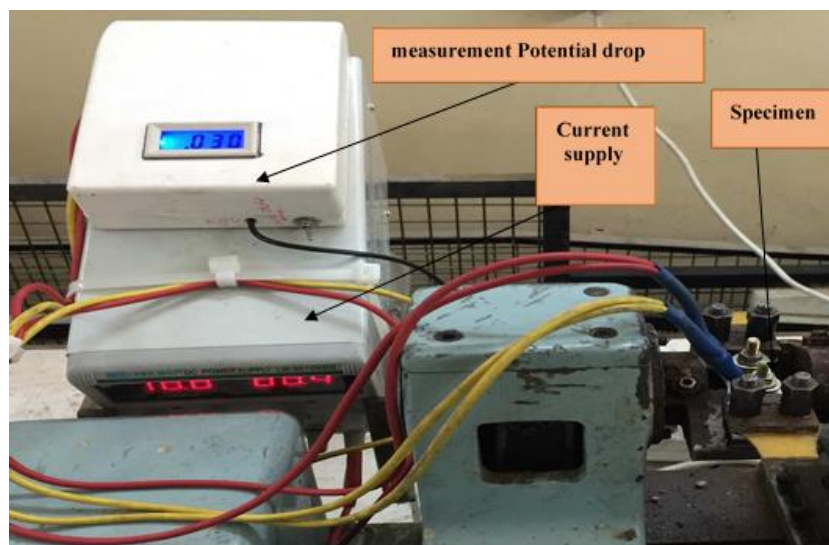
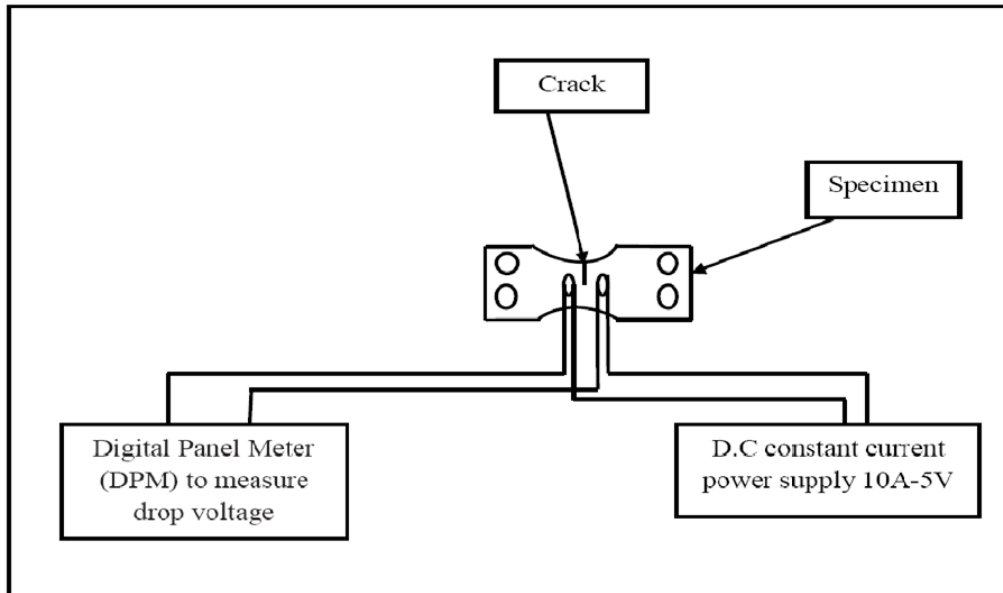
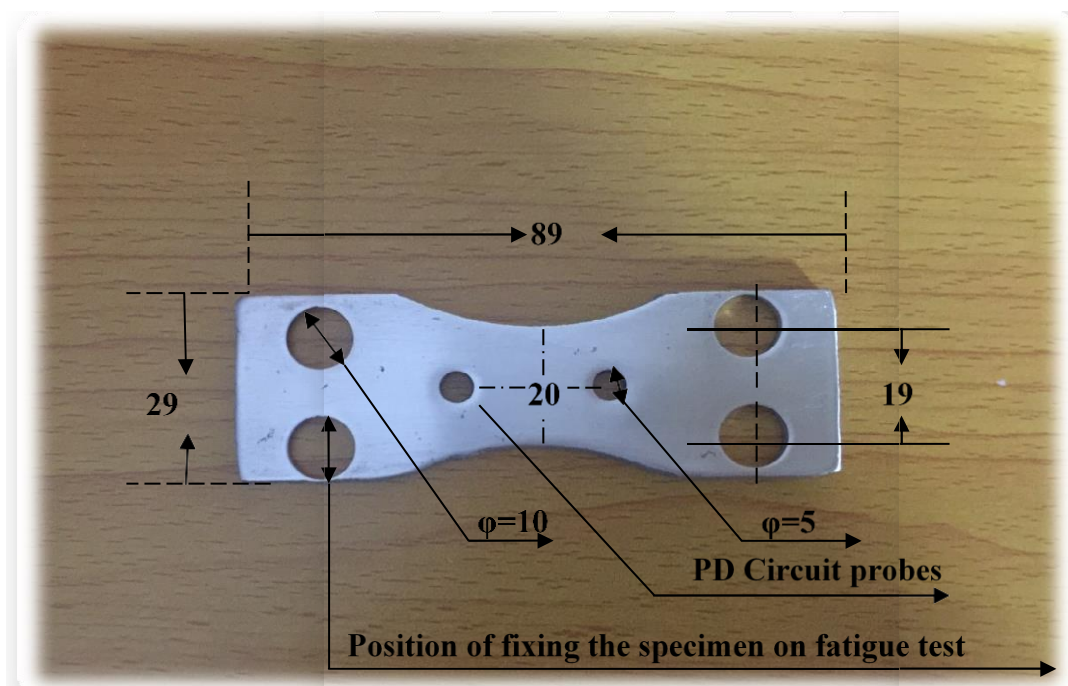


Figure 1. Potential drop device fixed on fatigue specimen

The voltage drop across the crack will increase as the crack length increases with a steady current flow. Low voltages were calculated using the electrical potential drop process. To test the voltage drop between two points, four probes were used. In two additional holes ($d=5\text{mm}$), four probes are applied to the specimens. Figure shows the 20mm gap between them (3), As seen in the diagram, two probes were used to add direct current (10A) and two probes were used to test drop voltage through the crack (2).

**Figure 1.** EPD Circuit Schematic**Figure 3.** ASTM D3479M-96 reference reverse cyclic bending fatigue test specimen of 3mm constant thickness (all measurements in mm).

Uniaxial tensile measurements create a nominally uniform strain field along the gauge length (up to the onset of necking), but the strain field is considerably more complicated by using the PD technique to calculate crack growth. To see if the same measurement methods would accurately forecast the impact of strain in such complicated strain fields, The study looked at monotonically filled specimens with a stationary crack. To decide how these variables affect the relationship between strain and PD, a variety of specimen geometries, crack lengths, and PD configurations are considered. In the following part, the experimental setup is outlined in detail, accompanied by descriptions of the FE analyses.

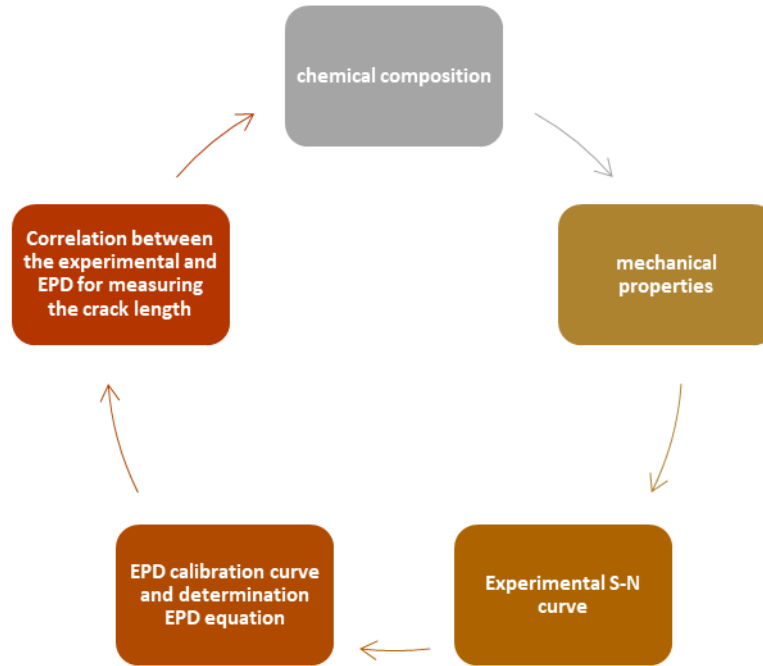


Figure 4. Flow chart of the experimental work

EXPERIMENTAL RESULTS AND DISCUSSION

The aim of the experiment is to use EPD to detect and quantify crack duration and compare the findings to the experimental the substance under investigation was 7075-T6 Al-alloy in the form of rolled sheets, with the chemical composition described in weight percentages in table (1). The State Company for Inspection and Infrastructure Rehabilitation (S.I.E.R), labs, and engineering research department in Baghdad/Iraq conducted an experimental study of chemical analysis using spectrum analyses. The mechanical properties are shown in the table below (2). Both specimens were machined parallel to the rolling trajectory on both sides. The tensile test specimen is illustrated in figure (5) according to (ASTM D-638-I) standard. Fatigue Strength 186MPa measured at 107 cycles.

Table 1. Chemical composition of 7075-T6 in wt%

| Component | % Si | % Fe | % Cu | % Mn | % Mg | % Cr | % Zn | % Ti | % other | % Al |
|-------------------------|-------|-------|---------|-------|---------|-----------|---------|-------|---------|------|
| Standard ASTM E1251- 11 | ≤ 0.4 | ≤ 0.5 | 1.2-2.0 | ≤ 0.3 | 2.1-2.9 | 0.18-0.28 | 5.1-6.1 | ≤ 0.2 | ≤ 0.15 | Rem. |
| Experimental (S.I.E.R) | 0.26 | 0.24 | 1.81 | 0.11 | 2.15 | 0.183 | 5.52 | 0.028 | 0.089 | Rem. |

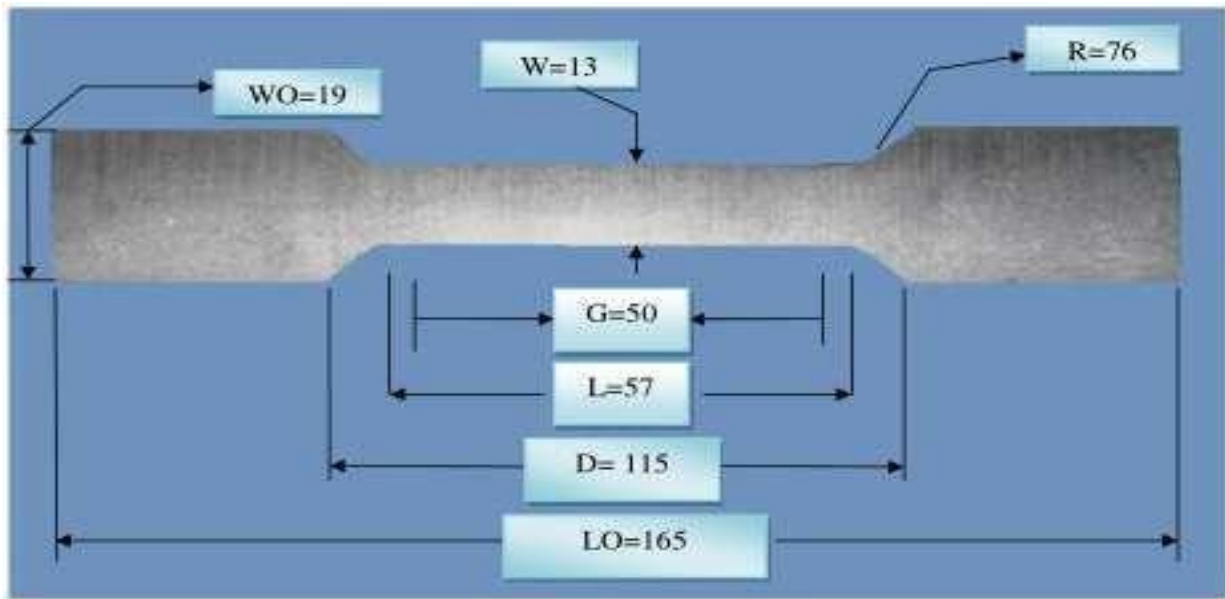


Figure 5. Standard tensile test specimen

Table 2. Mechanical properties of 7075- T6

| Mechanical Properties | Experimental | Standard (ASTM B557M - 15) |
|---------------------------|--------------|-----------------------------|
| Hardness , Rockwell B | 90 | 87 |
| Ultimate Tensile Strength | 502 MPa | 572 MPa |
| Tensile Yield Strength | 406 MPa | 503MPa |
| Elongation at Break | 12% | 11% |
| Modulus of Elasticity | 74 GPa | 71.7 GPa |
| Poisson's Ratio | 0.33 | 0.33 |
| Fatigue Strength | 186 MPa | 195 MPa |

The specimens were subjected to fatigue bending tests with a steady amplitude. At room temperature, with a stress ratio of $R=-1$, in stress management. A total of 15 specimens are examined to calculate the S-N curve. In the diagram, the experimental S-N curve data of 7075-T6 Al alloy is plotted (6). *R2 is a hand measure of the quality of fit [18].

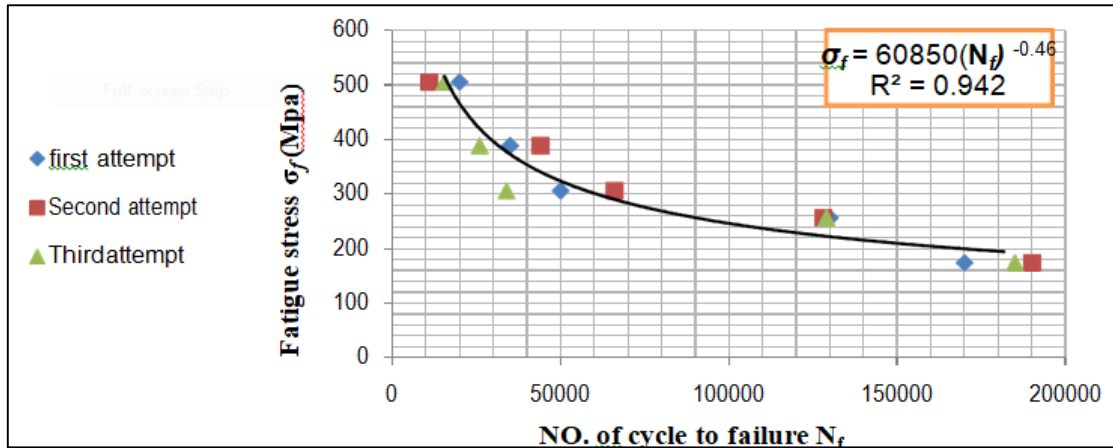


Figure 2. Relationship between applied stress and No. of cycle to failure(Nf)

Table 1. Experimental S-N curve data

| (Crack length) (a)mm | N (cycles) | da/dN mm/cycles | aav (mm) |
|-------------------------|---------------|--------------------|-------------|
| Applied stress 200 MPa | | | |
| 6.2 | 128000 | 4.843 | 3.1 |
| 14.5 | 217600 | 9.263 | 4.15 |
| 16.4 | 288000 | 2.698 | 0.95 |
| 17.9 | 310000 | 6.818 | 0.75 |
| Applied stress 300 MPa | | | |
| 6.2 | 40000 | 1.55 | 3.1 |
| 8.4 | 60000 | 1 | 1 |
| 12.7 | 80000 | 2.15 | 2.15 |
| 16 | 100000 | 1.65 | 1.65 |
| Applied stress 400 MPa | | | |
| 7.1 | 18000 | 3.944 | 3.55 |
| 11 | 26000 | 4.875 | 1.95 |
| 15 | 31000 | 8 | 2 |
| 17.6 | 34000 | 8.667 | 1.3 |

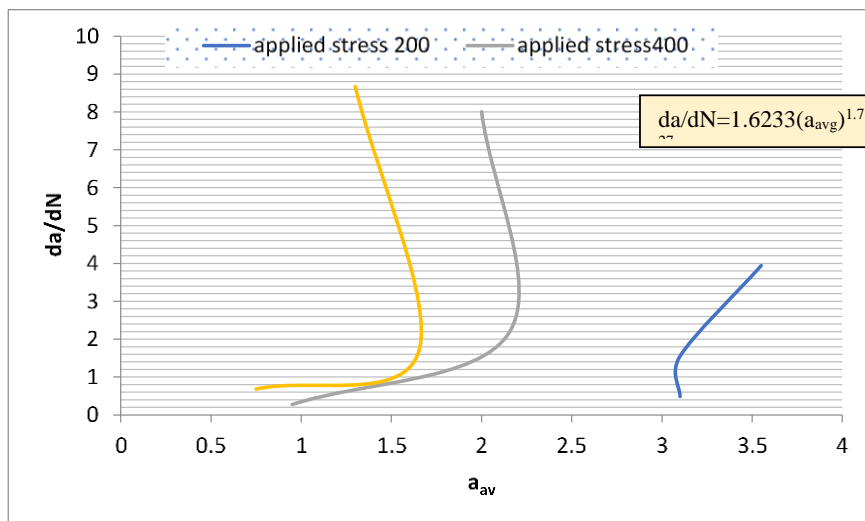
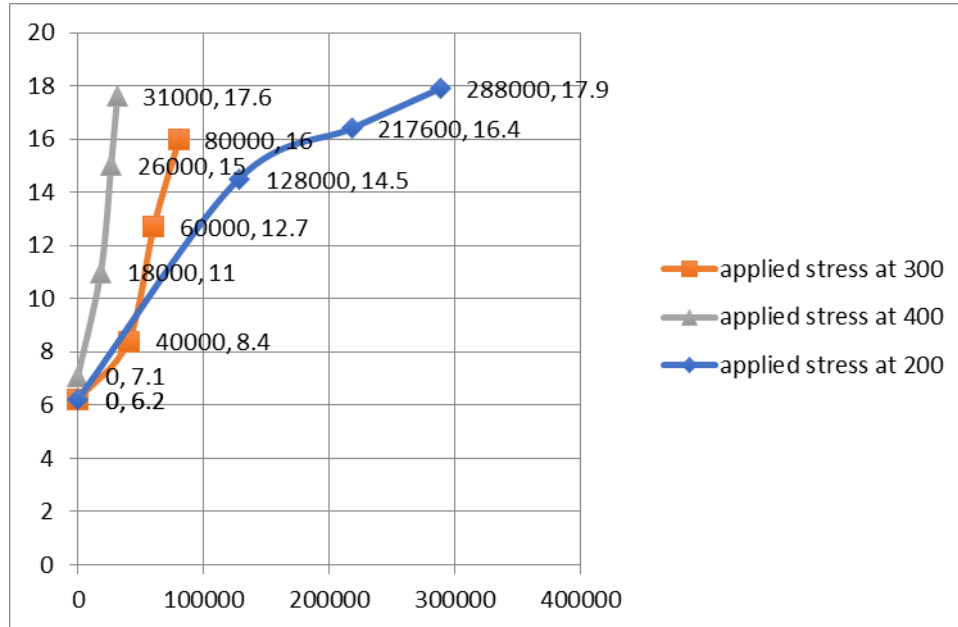


Figure 3. Results for aavand da/dN for7075-T7351

The crack growth rate derived from regression analysis is shown in fig(7). All of the evidence points to good crack development. The crack growth rate can be expressed as a function of crack size if there is a link between crack length and growth rate. To determine the link between the crack's length and its rate of development. The data demonstrate that when the crack size grows larger, the growth rate slows.

**Figure 8.** Results for crack length vs. number of cycles for7075-T7351

The crack growth rates are monotonically increasing. This indicates that for a given applied load, the applied stress intensity factor increases with fracture length. The baseline specimen behaves like most ordinary metallic samples, with cracking beginning at the machined notch tip and progressing to failure over time [19]. When calculating the fracture strength of a material with a crack, the critical stress intensity factor is applied. The critical stress intensity factor of a ductile material, unlike certain other material characteristics such as elastic modulus, is not a constant value but fluctuates with the thickness of the material. In the application of linear elastic fracture mechanics (LEFM) theory to practice, the stress intensity factor (SIF) is the most important element. It's useful for determining if a machine or structural component with a fracture is safe or reliable. It allows you to calculate the crack development rate of a component under fatigue loading, stress corrosion, and other conditions. The stress intensity range is estimated when a cyclic load is given to a material, as explained in the section:

$$\Delta K = \Delta \sigma \sqrt{\pi a_{av}} \quad (1)$$

ΔK : Stress intensity factor range

$\Delta \sigma$: Applied stress in MPa.

a_{av} : crack length in mm.

The most widely accepted formula is the Paris equation, which was proposed in the early 1960s. In this equation

$$da/dN = A(\Delta K)^B \quad (2)$$

The SIF related to the stress on the component and the fracture toughness of its material are required for the safety evaluation. The latter is experimentally collected material data. In some cases, the former can be obtained through SIF handbooks, Because of their versatility and ability to handle complicated geometries with ease, numerical techniques have been frequently used. The finite element method, the boundary element method, and the matrix method are the three most important numerical approaches [20]. Strain gauge based approach,

photoelasticity, and caustics method are some of the experimental approaches used. Sih and Atluri have compiled excellent accounts of analytical and finite element based approaches.

Table 4. Stress intensity factor range for 200MPa

| $\Delta\sigma$ | ΔK | da/dN |
|----------------|------------|-------------|
| 400 | 2628.307 | 4.84375E05 |
| 400 | 2858.736 | 9.26339E-05 |
| 400 | 2935.33 | 2.69886E-05 |
| 400 | 2998.826 | 6.81818E-05 |

Table 2. Stress intensity factor range for 300MPa

| $\Delta\sigma$ | ΔK | da/dN |
|----------------|------------|----------|
| 600 | 3498.082 | 0.000155 |
| 600 | 3738.888 | 0.00011 |
| 600 | 3672.797 | 0.000215 |
| 600 | 3584.533 | 0.000165 |

Table 3. Stress intensity factor range fo 400MPa

| $\Delta\sigma$ | ΔK | da/dN |
|----------------|------------|-------------|
| 800 | 5046.948 | 0.000394444 |
| 800 | 5404.275 | 0.0004875 |
| 800 | 5723.328 | 0.0008 |
| 800 | 5947.181 | 0.000866667 |

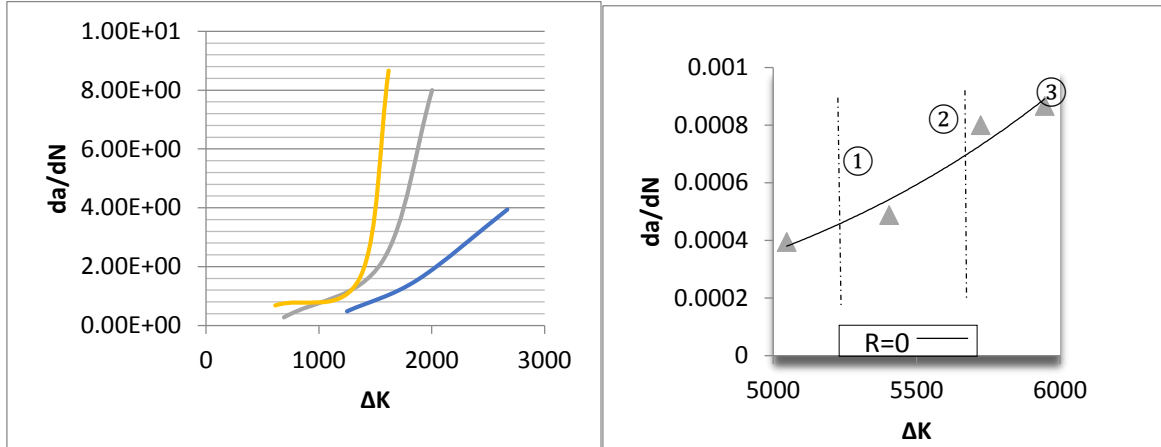


Figure 9. Relationship between Stress intensity factor range and da/dN

Table 7. Paris Equation coefficients

| Applied stress | 200 MPa | 300 MPa | 400 MP |
|----------------|---------|---------|--------|
| A | 1E-09 | 5E-09 | 6E-07 |
| B | 2.7588 | 2.6909 | 2.1478 |

The data is presented in Fig(9) as the rate of crack growth per loading cycle (a/N or da/dN) versus the variability of the stress-intensity factor at the crack tip (KI). The mechanical driving force is represented by KI, which

takes into account the influence of changing crack length as well as the degree of cyclic loading. The potential drop technique works on the idea that every surface fracture in a conducting specimen creates a disruption in the flow of electric current around the fracture, resulting in a quantifiable change in potential across the fracture. A continuous current is sent through a specimen in this procedure. With a rise in current path resistance and potential, the minimum width of the specimen or the minimum cross-sectional area of the specimen decreases as the crack lengthens. The experimental calibration curve results are provided in this paper as a possible drop ratio vs surface crack length. The growth rate curve usually has tails at the top and lower ends. For tiny values of K, the tail at the lower end approaches a vertical asymptote known as the fatigue fracture development threshold. For stress intensity levels below the threshold, crack development is uncommon.

For large values of K, the tail of the curve approaches a vertical asymptote as well. The vertical asymptote in the upper region of the graph represents the critical stress intensity for the material when the stress intensity ratio R is equal to 0, corresponding to zero-to-tension loading. Keep in mind that heavy areas will require more time to complete. The fracture grows at a certain rate due to varying stress intensity. When a given stress intensity range K is applied to a material for a certain number of cycles N, the fracture lengthens by a given amount a. The ratio a/N is then used to calculate the fracture growth rate over a specified stress intensity range. The derivative da/dN gives the fracture development rate in continuous form. The majority of current LEM applications to describe crack growth behavior are linked to Region II. The da/dN versus log ΔK curve is nearly linear in this region, and it lies between and There have been many curve fits proposed for this region. The most widely accepted formula is the Paris equation, which was proposed in the early 1960s. In this equation

$$da/dN = A(\Delta K)^B$$

$$Nf = \int_{a_i}^{a_f} \frac{da}{(\Delta k)^B} = \int_{a_i}^{a_f} \frac{da}{A(\sigma_A \sqrt{\pi a})^B} = \int_0^{18} \frac{1}{A(\sigma_A \sqrt{\pi a})^B} \frac{da}{a^{\frac{B}{2}}} \tag{3}$$

The initial crack length is a_i , while the final (critical) crack length is a_f . Using the formula from Paris . Because A, B, and σ_A are all constants, the only variable is a, and integration is simple, yielding.

$$Nf = \frac{a^{1-\frac{B}{2}}}{A(\sigma_A \sqrt{\pi})^B (1-\frac{B}{2})} \tag{4}$$

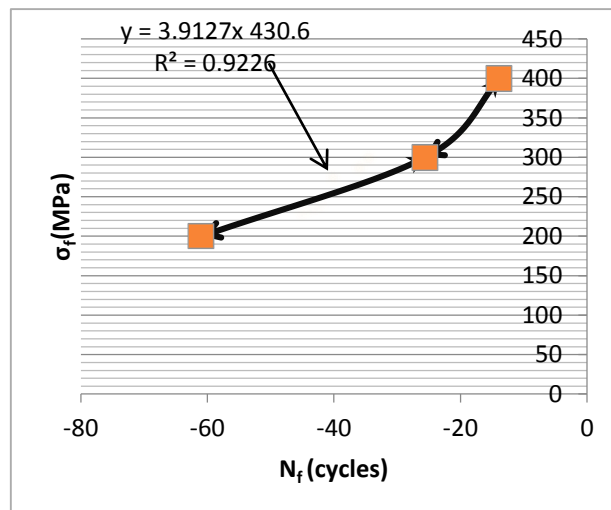


Figure 10. The S-N curve after EPD

The maximum load and stress ratio are the primary determinants of a fatigue crack's development or extension under cyclic loading. However, as with fracture initiation, a variety of other parameters, including as the environment, frequency, temperature, and grain orientation, can have a significant impact. Fatigue crack

propagation testing generally entails cycling of notched specimens that have been precracked in fatigue at a constant load amplitude. Crack length is calculated as a function of elapsed cycles, and the rate of crack development, da/dN , is calculated using numerical analysis. Crack growth rates are calculated as a function of the range of crack tip stress-intensity factors, ΔK . By comparing the S-N curves of notched and unnotched specimens, the influence of notches on fatigue strength may be assessed. The information for notched. Typically, specimens are plotted in terms of nominal stress depending on the specimen's net cross section. The fatigue-notch factor, K_1 , measures how effective the notch is at lowering the fatigue limit. The ratio of the fatigue limit of unnotched specimens to the fatigue limit of notched specimens is used to calculate this factor. Materials that do not show signs of fatigue. The fatigue-notch factor is determined by the fatigue strength after a certain number of cycles.

Table 8. Correlation between actual crack length and crack calibration

| Applied stress σ_f | No.of average cycle to failure, N_{favg} | EPD prediction (crack length) at failure mm | Actual crack length at failure mm | |
|---------------------------|--|---|-----------------------------------|-----|
| 200 | 235900 | 13.75 | 16.3 | 15% |
| 300 | 70000 | 10.8 | 11.4 | 5% |
| 400 | 27250 | 12.7 | 14.2 | 11% |

The accompanying table (8) shows that the magnitude of any future change in PD is proportional to the extent of crack formation. In general, the anticipated crack length and the measured crack length are rather close [20]. used the PD technique to determine the fracture length in C-M structural steel. They discovered that the projected fracture length was always shorter than the observed crack length in experiments, and this conclusion was confirmed in the current study. The aforementioned data also indicate the imposed stress level. Increasing the applied stress decreases the ultimate fracture length or lowers the EPD method output reading.

CONCLUSIONS

The effects of electrical PD on the fatigue crack development behavior of aluminum alloy (AA) 7075-T7351 sheets were studied. For two distinct crack configurations, the effects of the electrical PD approach on fatigue crack development were studied and analyzed. The use of electrical PD method resulted in a considerable reduction in fatigue fracture development rates, according to a comprehensive analysis of the various electrical PD method impacts. The majority of cracks were discovered at 20% of the overall fatigue life, suggesting that the remaining 70% of the fatigue life was dominated by long cracks or fracture propagation. The electrical potential drop approach provided a quick means of calibrating fatigue fracture length measurements. The electrical potential calibration curve allows for precise fatigue fracture length measurement utilizing the EPD technique. EPD predicts crack lengths that are always less than the actual crack length.

REFERENCES

- [1] S. Datta, A. Chattopadhyay, N. Iyyer, N. Phan, "Fatigue crack propagation under biaxial fatigue loading with single overloads", *Int. J. Fatigue.*, Vol. 109, Pp. 103–13, 2018.
- [2] R.K. Neerukatti, S. Datta, A. Chattopadhyay, N. Iyyer, and N. Phan, "Fatigue crack propagation under in-phase and out-of-phase biaxial loading", *Fatigue Fract Eng Mater Struct.*, Vol. 41, Pp. 387–99, 2018.
- [3] A. Fatemi, N. Gates, D.F. Socie, N. Phan, "Fatigue crack growth behaviour of tubular aluminium specimens with a circular hole under axial and torsion loadings", *Eng Fract Mech.*, Vol. 123, Pp. 137–47, 2014.
- [4] K. Tanaka, "Crack initiation and propagation in torsional fatigue of circumferentially notched steel bars", *Int J Fatigue*, Vol. 58, Pp. 114–25, 2014.

- [5] J.M. Lowes, G.D. Fearnehough, "The detection of slow crack growth in crack opening displacement specimens using an electrical potential method", *Eng Fract Mech.*, Vol. 3, Pp. 103-104, 1971. [10.1016/0013-7944\(71\)90002-6](https://doi.org/10.1016/0013-7944(71)90002-6)
- [6] A. Bakker, "A DC potential drop procedure for crack initiation and R-curve measurements during ductile fracture tests", *ASTM STP*, Vol. 856, Pp. 394-410, 1985.
- [7] B.L. Freeman, G.J. Neate, "The Measurement of crack length during fracture at elevated temperatures using the D. C. potential drop technique", In: Beevers CJ, editor. *Meas. Crack Length Shape Dur. Fract. Fatigue*, Engineering Materials Advisory Services Ltd.; 1980.
- [8] T. Kuno, M. Shimizu, K. Yamada, M. Tamura, "Endurance limit and threshold condition for microcrack in steels", 2nd International conference on fatigue thresholds, Pp. 817-826, 1984.
- [9] Klima S. J. , Fisher D.M. , Buzzard R.J "Monitoring crack extension in fracture toughness tests by ultrasonic" *Journal of Testing and evaluation*, vol.4, Nov. PP.397- 404,1976.
- [10] S.J. Klima, D.M. Fisher, R.J. Buzzard, "Monitoring crack extension in fracture toughness tests by ultrasonic", *Journal of Testing and evaluation*, Vol. 4, Pp. 397- 404, 1976.
- [11] D.T. Read and M. PFUFF, "Potential drop in the center-cracked panel with asymmetric crack extension", *International Journal of Fracture*, Vol. 48, No. 3, Pp. 219-229, 1991.
- [12] E. Madhi, P.B. Nagy, "Sensitivity analysis of a directional potential drop sensor for creep monitoring", *NDT and E International*, 2011.
- [13] M. Verstraete, S. Hertelé, W.D. Waele, R. Denys, and K.V. Minnebrugge, "Measurement of ductile crack extension in single edge notch tensile specimens)", *International Conference on Experimental Mechanics*, PAPER REF, Pp. 2876, 2012.
- [14] M. Saka, H. Tohmyoh, T. Suzuki, and S.R. Ahmed, "Potential drop imaging technique for sensitive NDE of small surface cracks", *Asia-Pacific Conference on NDT*, 2006.
- [15] J.J.A. van Kuijk, R.C. Alderliesten, R. Benedictus, "Measuring crack growth and related opening and closing stresses using continuous potential drop recording", *Engineering Fracture Mechanics*, 2021.
- [16] C.R. Paul, S.A. Nasar "Introduction to electromagnetic fields, second ed". McGraw-Hill, 1987.
- [17] K. Tarnowski, C.M. Davies, K.M. Nikbin and D. Dean, "The influence of strain on crack length measurement using the potential drop technique," In 16th International Conference on Experimental Mechanics, Cambridge, UK, Pp. 7-11, 2014.
- [18] M.B.H. Al-Khafaji, "Experimental and theoretical study of composite material under static and dynamic loadings with different temperature conditions," Phdthesis, university of technology, 2014.
- [19] J. Rushau, "Fatigue crack nucleation and growth rate behavior of laser shock peened titanium", *Int. J. Fatigue*, Vol. 21, Pp. S199-209, 1999.
- [20] J.M. Lowis, G.D. Fearnehough, "The detection of slow crack growth in crack opening displacement specimens using an electrical potential method", *Engineering Fracture Mechanics*, Vol. 3, Pp. 103-108, 1971.

